Colloid Polym Sci 276:232–238 (1998)

ORIGINAL CONTRIBUTION

P.C. Schulz
M.A. Morini
M.E. Gschaider de Ferreira

Aggregation effects on evaporation and the air/water interface of dodecyltrimethylammonium hydroxide solutions

Received: 9 January 1997
Accepted: 19 October 1997

P.C. Schulz (✉) · M.A. Morini
M.E. Gschaider de Ferreira
Departmento de Química
e Ingeniería Química
Universidad Nacionaldel Sur
Avda. Alem 1253
8000 Bahia Blanca
Argentina

Abstract The system dodecyltrimethylammonium hydroxide (DTAOH)–water was studied by surface tension, ion-selective electrodes and evaporation in an electrobalance. Results confirmed earlier conclusions about a stepwise aggregation mechanism in DTAOH solutions. The aggregation process started at a total concentration $C_T = (2.51 \pm 0.10) \times 10^{-4}$ mol dm^{-3}) which probably corresponds to the formation of dimers. At $C_T = (1.300 \pm 0.041) \times 10^{-3}$ mol dm^{-3} there was a change in the surface and evaporation behavior, corresponding to the formation of small, fully ionized aggregates which grew with increasing concentration. At $C_T = (1.108 \pm 0.010) \times 10^{-2}$ mol dm^{-3} the formation of true micelles with hydroxide counterions in the Stern layer did not change significantly the evaporation and adsorption behavior. This means that between this concentration and $C_T = (3.02 \pm 0.28) \times 10^{-2}$ mol dm^{-3}, the changes in structure were gradual. At the latter concentration there was a sudden change in the monolayer state at the air/water interface, with a strong surfactant desorption, and a major change in evaporation behavior. The changes are compatible with the formation of few, large aggregates reducing the total concentration of kinetically independent solute units, which in turn increased the activity of the solvent. This phenomenon is in agreement with literature information. The reduction in the evaporation rate of water was mainly due to the reduction of the water activity, caused by colligative effects. The reduction of the effective area available for evaporation had only a slight effect in water evaporation.

Key words Dodecyltrimethylammonium hydroxide – soluble monolayer – air/water interface – evaporation – ion-selective electrodes

Introduction

In a previous paper, we have found that the combination of surface tension and ion-selective electrodes measurements enables the state of the adsorbed monolayer of soluble surfactants to be studied [1]. We have also found that the transformations in structure of aggregates in the bulk phase affect the structure and properties of the air/water adsorption monolayer and the evaporation behavior of the solution. The aggregation behavior of dodecyltrimethylammonium hydroxide (DTAOH) in aqueous solution follows a stepwise mechanism [2]. The several steps in the aggregation process have been studied here to obtain new information about the phenomena occurring at the surface and in the bulk.

We also studied the evaporation through the monolayer to confirm that soluble monolayers do not influence

significantly the evaporation behavior of the solution, as stated in literature [1, 3].

Experimental

The preparation of DTAOH solutions has been described elsewhere [4]. The solutions were prepared by dilution of the concentrated solution with double-distilled CO_2-free water. Much care was taken to avoid contamination by atmospheric CO_2 in this work [2].

The statistical treatment of data was performed by the least-squares method, using a Student's t-distribution and a confidence level of 0.90.

The surface tension measurements were performed with a Du Noüy (Krüss) tensiometer, thermostatted at $25.0 \pm 0.1\,^{\circ}C$.

Dodecyltrimethylammonium ion (DTA^+) activity measurements were performed with an ion-selective electrode which has been described elsewhere [2]. OH^- activity was determined with an Orion glass electrode. A CRIBBAB pH-meter and millivoltmeter was employed. The treatment of potentiometric data has been described elsewhere [2].

The evaporation rate measurements were performed in a CAHN 1000 electrobalance, operating in a register range of 1000 mg and an output potential of 10 mV. The pressure was 101.325 kPa. The samples were measured at $25.0 \pm 0.1\,^{\circ}C$, thermostatted with water circulation. Known volumes of the solutions were poured into pyrex cylindrical containers with a 2.9 cm internal diameter. To avoid secondary Archimedes effects, a compensator container was hung on the other arm of the electrobalance. The thermocouple (Fe-constantan) was in contact with the solution through a thin glass sheath. The electrobalance measured directly the loss of weight of the solution with time.

To determine the surface excess at the air/water interface (Γ) the Gibbs adsorption isotherm in its general form for multicomponent systems has been employed:

$$d\sigma = -\sum_i \Gamma_i \, d\mu_i \,, \tag{1}$$

where σ is the surface tension (mN/m) and μ_i the chemical potential of component i. The studied system had two components in the phase rule sense: water and DTAOH. The adsorbable species are OH^- and DTA^+. Since the temperature is constant, the system had only one degree of freedom, that is, the concentration of one of its components. We have taken the DTAOH concentration as the degree of freedom. This gives

$$d\sigma = -\Gamma \, d\mu \,, \tag{2}$$

with $d\mu = RT\, d(\ln a)$, in which a is the activity of the adsorbable component in the bulk phase. Only the monomeric form of the surfactant contributes to the surfactant activity or chemical potential, and hence to the tension reduction [5]. In the studied system, only free (nonmicellized) DTA^+ ions may adsorb at the air/water interface. Micelles are not surface-active (6), and are excluded from the interface region [7]. The adsorbable species has been taken as the whole DTAOH molecule. Notice that in fully ionized, not micellized salts,

$$a_{salt} = a_+ a_- = (a_\pm)^2$$

and hence $\ln a_{salt} = \ln(a_\pm)^2 = 2\ln a_\pm$. This is the origin of the coefficient used in the Gibbs equation when the adsorbable species is ionized (alternatively, it may be explained by equal adsorption of cations and anions in order to maintain charge neutrality). The use of $\ln a_{salt}$ is completely equivalent to that of $2\ln a_\pm$. In the usually studied systems, $c = c_+ = c_-$, and this situation leads to the use of the latest form. In the system DTAOH–water, $[OH^-] \neq [DTA^+]$ at concentrations above the cmc. The base DTAOH is strong enough to consider it as fully ionized ($pK_b = 2.89$) [3]. Then, the chemical potential of the bulk unmicellized surfactant is

$$\begin{aligned}\mu_{\text{unmicellized species}} &= \mu_{\text{ionised surfactant}} = \mu^\circ_{\text{ionised surfactant}} \\ &+ RT \ln a_{\text{ionised surfactant}} = \mu^\circ_{DTA} + RT \ln a_{DTA^+} \\ &+ \mu^\circ_{OH^-} + RT \ln a_{OH^-} = \mu^\circ_{DTA^+} + \mu^\circ_{OH^-} \\ &+ RT \ln a_{OH^-} a_{DTA^+} \,.\end{aligned}$$

Then,

$$d\mu_{\text{unmicellized species}} = RT\, d\ln a_{OH^-} a_{DTA^+} = 2\, d\ln(a_\pm) \,.$$

Then the prefactor in the Gibbs equation was included in the definition of the activity of the adsorbable species. We did not use the form $2\, d\ln(a_\pm)$ because $a_{OH^-} \neq a_{DTA^+}$ at concentrations above the cmc. Then,

$$\Gamma = -\frac{1}{RT}\frac{d\sigma}{d\ln a} \,, \tag{3}$$

where $a = a_{OH^-} a_{DTA^+}$ is the bulk activity of the adsorbable species, a_{OH^-} and a_{DTA^+} being the activities of free (unmicellized) OH^- and DTA^+ ions.

The total surface concentration was computed by

$$C^s = [DTAOH]_{free}\delta + \Gamma \,, \tag{4}$$

where δ is the monolayer thickness. The value of $\delta = 3.75$ nm was taken as that of the dodecyltrimethylammonium bromide, which was determined from neutron

reflectivity measurements by Lu et al. [8]. The surface area per adsorbed molecule is

$$A_{\text{molec}} = \frac{1}{C^{s} N_{A}}, \tag{5}$$

N_A being the Avogadro's number.

Results

Surface monolayer

The activities of the free OH^- and DTA^+ ions in solution are shown in Fig. 1, together with the total activity a of free DTAOH vs. the total surfactant concentration (C_T). In Fig. 2, the surface tension vs. total concentration data has been plotted, showing the concentrations at which different steps of the aggregation process occur [2]. These points will be discussed in detail in the Discussion section.

Fig. 1 Activity of (○) free DTA^+ (△) free OH^- (□) free DTAOH vs. total concentration of surfactant (C_T)

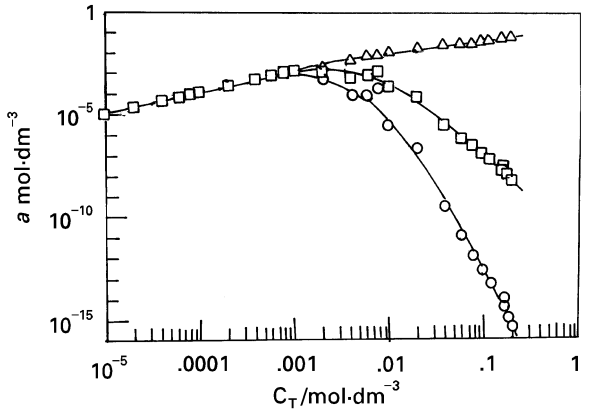

Fig. 2 Surface tension vs. total concentration of surfactant

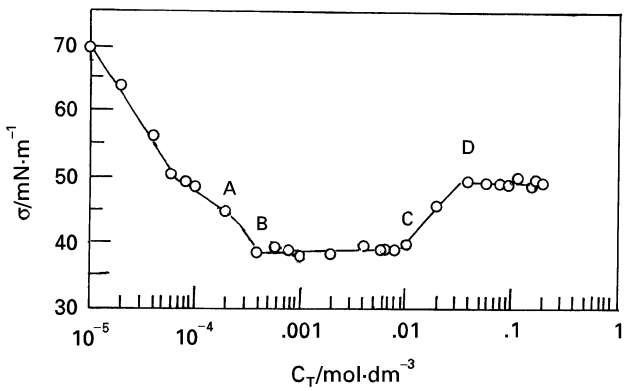

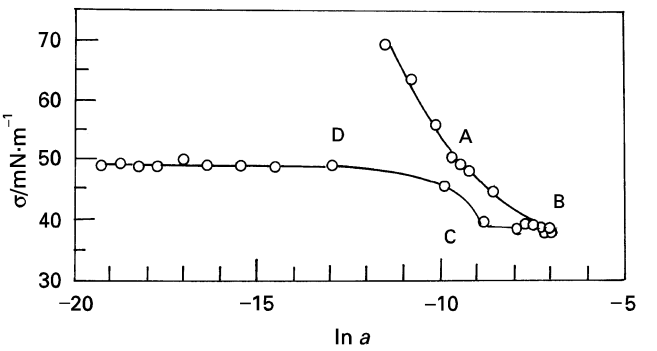

Fig. 3 Surface tension vs. total activity of monomeric species

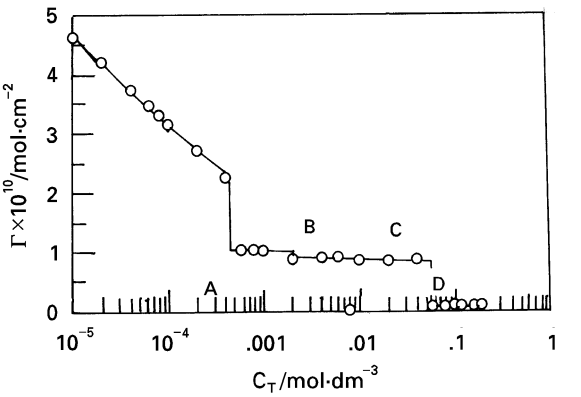

Fig. 4 Surface excess vs. total concentration of surfactant

In Fig. 3 the surface tension is shown as a function of the activity of free DTAOH. By using the Gibbs equation, Γ was computed and plotted vs. the total concentration in Fig. 4.

The values of A_{molec} have been plotted in Fig. 5. Figure 6 shows the plot of ΠA_{molec} vs. Π, where $\Pi = \sigma_0 - \sigma$ is the surface pressure. The ideal value $kT = 4\ \text{mN nm}^2/\text{m}$ is also shown.

Evaporation

The loss of weight (in kg per square meter per second) gave curves following parabolic equations with the time having the general form [9]

$$v = v_0 - Kt^{1/2}, \tag{6}$$

where v and v_0 are the rate of evaporation at the time t and the initial evaporation rate, measured in loss of mass per square meter per second. The values of v_0 and K were found by the least-squares linear regression method using

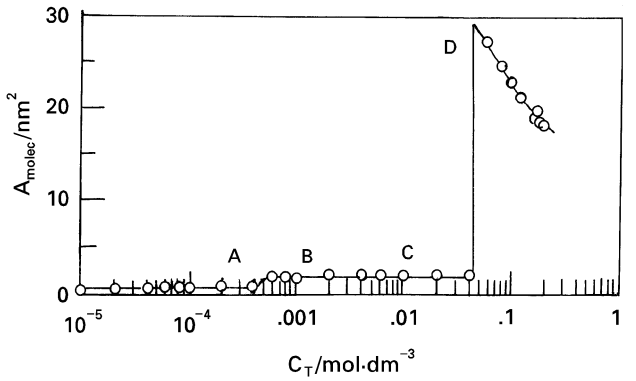

Fig. 5 Area per molecule vs. total concentration of surfactant

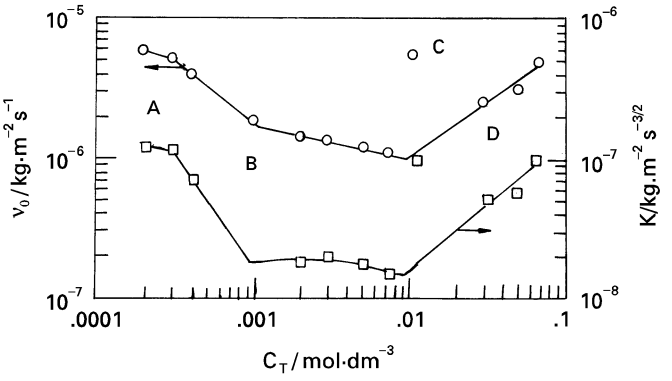

Fig. 7 Vaporization data for DTAOH aqueous solutions: (○) v_0, (□) K

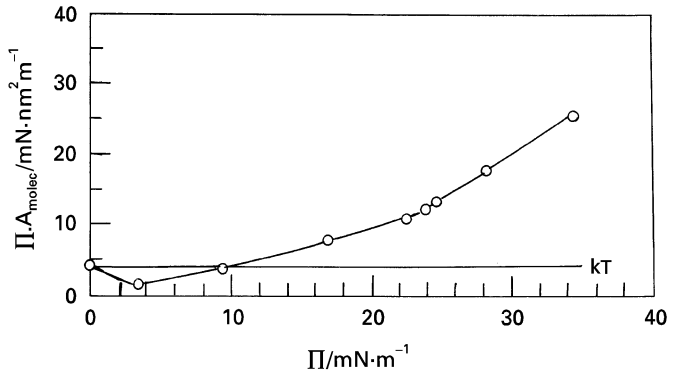

Fig. 6 Plot of ΠA_{molec} vs. Π. The horizontal straight line at $kT = 4$ mN (nm^2)/m is the ideal bidimensional gas behavior

Eq. (5) and the experimental data, and they are shown in Fig. 7.

Discussion

Surface monolayer

In Fig. 4 it may be seen that there is a monotonic reduction of the surface excess with increasing total concentration, showing very marked steps at concentrations A and D, and a slight step at concentration B. The point A ($C_T = (2.51 \pm 0.10) \times 10^{-4}$ mol dm^{-3}) was of uncertain interpretation in the process of aggregation, probably the starting of dimers formation. Point B ($C_T = (1.300 \pm 0.041) \times 10^3$ mol dm^{-3}) corresponds to the formation of small, fully ionized aggregates which grew with increasing concentration. Point C ($C_T = (1.108 \pm 0.010) \times 10^{-2}$ mol dm^{-3}) corresponds to the formation of true micelles (cmc) in which the counterions joined the micelle surface, and point D ($C_T = (3.02 \pm 0.28) \times 10^{-2}$ mol dm^{-3}) corresponds to a change in the micelle structure [2]. At low concentrations the increase in the bulk activity with total concentration was more pronounced than that at the surface. This reduced the difference between them, giving a decrease of Γ with increasing total concentration.

In Fig. 5 it may be seen that at very low total concentration, when only monomeric DTA^+ and OH^- ions were present, the surface area per adsorbed molecule (A_{molec}) increased very slowly from 0.36 to 0.52 nm^2 near point B. Between points A and B there was a desorption and A_{molec} became 1.63 nm^2. This means that the aggregates had a slight energetic advantage compared with the previous monomeric and dimeric bulk structures. The complete ionization of the polar headgroups minimizes the hydrophobic bound influence. For dimers, the hydrophobic bound effect per methylene group is about half of the value for micelles [10], and this energetic advantage might play a role in the desorption near point B.

There was a gradual increase of A_{molec} from B to C (from 1.63 to 1.92 nm^2) which indicates that the thermodynamic stability of the aggregates increased slightly with concentration (and with increasing size). At point C the aggregates captured OH^- counterions, but remained strongly ionized ($\alpha \approx 0.8$) [2]. Between points C and D, the increase in A_{molec} followed the previous tendency. The ionization degree (α) decreased to about 0.6 at point D [2], in which a change in the micelle structure occurred [2]. The change in structure was accompanied with a strong desorption, A_{molec} going to 27.1 nm^2, followed by a gradual decrease up to 18.1 nm^2 at the highest total concentration studied in this work (≈ 0.2 mol dm^{-3}).

Figure 6 shows that the monolayer formed at concentrations below point B had a strongly nonideal behavior, with A_{molec} values compatible with the bidimensional expanded liquid state [11–13]. Frumkin [14] found this type of nonideality in a series of fatty acid monolayers. Lucassen-Reynders [15] suggested that this nonideality is

mainly due to the interaction among hydrocarbon chains, and nonideality is expected when the chains are close to each other.

The other monolayers are compatible with strongly nonideal bidimentional gaseous states.

The radius of the unmicellized trimethylammonium headgroup was computed from data of Refs. [16–19] giving $r = 0.2643 \pm 0.0040$ nm. Using the hard disc model [20] the excluded area per surfactant molecule was computed by

$$A_0 = 2\pi r^2 , \tag{7}$$

giving $A_0 = 0.4389 \pm 0.0066\ \mathrm{nm}^2$. This value is only slightly smaller than the minimum value found in this system, $A_{\mathrm{molec}} = 0.52\ \mathrm{nm}^2$ and indicates that the lowest C_T monolayer is probably the most compact possible. In other systems it has been found that the polar headgroups remained hydrated at the interface [21]. This means that each polar headgroup had about 40 water molecules [22].

There was a series of simultaneous equilibria in the system at $C_T > A$:

$$\mathrm{nDTA^+} + \mathrm{mOH^-} = \text{aggregates} , \tag{8}$$

$$\mathrm{DTA^+} + \mathrm{OH^-} = \text{monolayer} . \tag{9}$$

It is obvious that the increase in stability of the aggregates will reduce the activity of free DTAOH, which in turn will reduce the surface concentration, giving an increased value of A_{molec}. Thus, the changes in A_{molec} which occurred at points A, B, C and D were probably due to an increased thermodynamic stability in the aggregates which started to form at the mentioned points. The growing of the bulk aggregates must be accompanied by a reduction in hydrocarbon/water contact. Since in soluble monolayers there is some immersion of the hydrocarbon chains into the water layer, ranging from 10% to 30% of the total chain length [4, 21, 23–30], the increasing compactness of the aggregates' structure produced an increased energetic advantage of the aggregates compared with the adsorbed monolayer. This advantage rose gradually up to point D. At that point there was a sudden increase in A_{molec}. The explanation is that at point D a major change in the aggregates structure occurred, whereas at concentrations below D, the changes were slight gradual modifications. This conclusion is in agreement with previous studies on this system [2].

It must be noticed that this situation is not common. There are some determinations of adsorption at concentrations above the cmc, mainly obtained by neutron reflectivity. For SDS, A_{molec} is constant and amounts $0.415\ \mathrm{nm}^2$ [31]. The same result was obtained by radioactive tracers [32]. Sasaki et al. [23] found that this situation remained unchanged up to about 20 mM and above this concentration A_{molec} increased. Tetradecyltrimethylammonium bromide solutions showed a decrease in A_{molec} above the cmc [7], but other measurements indicated an increase of about 15% between the cmc and 3cmc [33], similar to our results below point D.

Evaporation

The reduction in the initial rate of evaporation v_0 may be due to two different factors: one of them is an effect of reduction of the effective surface of water exposed to evaporation, because of the partial coverage of the air/water interface by surfactant molecules, the other is the reduction of water activity in the bulk, caused by the solutes.

Figure 7 shows a decrease in the initial evaporation rate at low concentrations between A and B. This decrease must be due to the increase of the bulk solute activity, accompanied by a decrease in water activity. The adsorbed surface layer did not have a noticeable effect, because of the almost constant value of A_{molec}. Since this value increased slightly in the same concentration range, its effect on v_0 might be the inverse of that observed.

Between B and C there was a slight decrease in v_0, which means that the total bulk solute activity increased with total concentration, but slower than at concentrations below B. This phenomenon is explained by the formation of aggregates, which reduced the number of independent solute particles in solution.

At point D, v_0 increased with concentration. This increase reflects the increase in water activity, because the formation of large aggregates with low surface charge significantly reduced the number of kinetically independent particles in solution.

By use of the hard disc model, the area occupied by a trimethylammonium headgroup was $A_{(\mathrm{CH_3})3\mathrm{N^+}} = 0.2195 \pm 0.0066\ \mathrm{nm}^2$. The surface available for water molecule is $A_{\mathrm{molec}}. - A_{(\mathrm{CH_3})3\mathrm{N^+}}$ per surfactant molecule, and the area per water molecule is $0.097\ \mathrm{nm}^2$ [34–39]. In this system, the mole fraction of water at the surface increased from 0.75 at point A to 0.95 immediately below point D, increasing suddenly to 0.996 at point D and then decreasing to 0.995 at the highest concentration studied. Then, if the surface coverage were the only hindrance for evaporation, the minimum value of v_0 might be 0.75 of the value for pure water ($(1.000 \pm 0.028) \times 10^{-5}\ \mathrm{kg/m^2\,s}$). It can be seen in Fig. 7 that the minimum value of v_0 is about $1 \times 10^{-6}\ \mathrm{kg/m^2\,s}$ at point C, in which it might be about $9.5 \times 1 \times 10^{-6}\ \mathrm{kg/m^2\,s}$ if the surface coverage were the main effect. The extra decrease in v_0 must be due to the reduction in water activity caused by the increase in the solute concentration.

The changes in slope at points A and B indicated changes in the manner in which the increase of C_T affected the activity of water. Between B and C, the formation of aggregates reduced the rate of increase of the solute activity, and in turn this reduced the decrease in water activity. The increase in v_0 above point D, changing the sign of the slope, indicated that the type of aggregates changed, giving fewer solute units and an increase of water activity. This is consistent with a sudden increase in the aggregates' size.

The variation in time of the evaporation rate (K) is related to the rate of diffusion of molecules with enough energy to evaporate, from the bulk to the surface, where the initial evaporation created a deficit of molecules having enough energy to evaporate [9]. The value of K is $(1.63 \pm 0.09) \times 10^{-7}$ kg/m s$^{3/2}$ in pure water. The reduction of K in surfactant solutions must be mainly due to steric hindrance to the diffusion of water in bulk solution. The evolution of K is almost parallel to that v_0. Since K is undoubtedly related to bulk solution properties, this evolution reinforces the conclusion that the evolution of v_0 is related to variations in bulk water activity, which is useful to interpret the changes in the structure of surfactant aggregates.

The effect of water activity changes on evaporation rate seem to be much larger than that on equilibrium vapor pressure. We have investigated other systems in which no surface active components were present. As an example, inverse micellar systems with Aerosol OT–Water-*n*-heptane [40]. We found a large decrease in evaporation rate of heptane, following the changes in the structure of inverse micelles in bulk. We are carrying out measurements on solutions of surface inactive electrolytes and the preliminary data indicated the same.

The analysis of all the above information supports the conclusion that DTAOH has a stepwise aggregation at four different concentrations (A, B, C and D), which has been found in previous work [2].

The presence of insoluble surfactant monolayers at the air/water interface affects the rate of transfer of solute gas molecules through the interfaces [41], reducing the evaporation of water [42, 43]. The reduction in mass transfer through a surfactant monolayer may be 5–25% from that of a clean surface of water [44]. Because surfactants reduce the rate of vaporization of small drops, their use has been proposed to reduce evaporation of fogs that protect crops from frost damage [45]. The effect has been explained by the solubility of water in the surfactant film and diffusion trough it to the air/liquid interface [46]. In a very recent work, Luckenheimer and Zembala [3] showed by osmometry that soluble surfactant monolayers do not affect the evaporation of water, except in the case of very compact monolayers. We have found the same situation in aqueous dodecanephosphonic acid solutions [1]. The results of this work reinforce the conclusion that soluble monolayers do not affect significantly the evaporation rate of water in surfactant solutions, in comparison with the changes in water activity due to colligative effects.

Conclusions

- The combination of surface tension and ion-selective electrodes measurements enables the adsorption of soluble surfactants above the cmc to be studied.
- This work supports the conclusion that DTAOH has a stepwise aggregation at four different concentrations (A, B, C and D), which has been found in previous work [2].
- The changes in aggregate structures below point D are gradual, whereas at point D there is a sudden change in structure which is reflected in major modifications in surface and evaporation properties.
- The reduction in the evaporation rate of water is mainly due to the reduction of the water activity, caused by the presence of solutes in bulk. The reduction in effective area available for evaporation has only a slight effect on water evaporation.

Acknowledgements One of us (M.A.M) has a fellowship from the Consejo Nacional de Investigaciones Científicas y Técnicas de la República Argentina. This work was supported by a grant from the Universidad Nacional del Sur.

References

1. Schulz PC, Minardi RM, Gschaider de Ferreira ME, Vuano B (1997) Colloid Polym Sci, in press
2. Schulz PC, Morini MA, Minardi RM, Puig JE (1995) Colloid Polym Sci 273:959
3. Lukenheimer K, Zembala M (1997) J Colloid Interface Sci 188(2):363
4. Morini MA, Minardi RM, Schulz PC, Puig JE, Hernandez-Vargas ME (1995) Colloids Surfaces A 103:37
5. Chang CH, Franses EI (1995) Colloids Surfaces A 100:1
6. Shaw DJ (1970) Introducción a la Química de Superficies y Coloides. Alhambra, Madrid
7. Lu JR, Simister EA, Thomas RK, Penfold J (1993) J Phys Chem 97:13907
8. Lu JR, Li ZX, Thomas RK, Penfold J (1996) J Chem Soc Faraday Trans 92(3):403
9. Schulz PC, Gschaider de Ferreira ME, Sierra GL (1995) Colloid Polym Sci 273:439

10. Mukerjee P, Mysels KJ, Dulin CI (1958) J Phys Chem 62:1390
11. Schukin ED, Pertsov AV, Amélina EA (1988) Química Coloidal. MIR, Moscow
12. Heimenz P (1977) Principles of Colloid and Surface Chemistry. Marcel Dekker, New York
13. Sakai H, Umemura J (1996) Chem Lett 465:123
14. Frumkin AN (1925) Z Phys Chem 116:466
15. Lucassen-Reynders EH (1966) J Phys Chem 70(6):1777
16. Tanaka M, Kaneshina S, Shin-No K, Okajima T, Tomida T (1974) J Colloid Interface Sci 46:132
17. Guvelli DE, Kayes JG, Davis SS (1981) J Colloid Interface Sci 82:307
18. Mukerjee P (1969) J Phys Chem 73(6):2054
19. Morini MA, Minardi RM, Schulz PC, Puig JE, Rodríguez JL, submitted
20. Janczuk B, Bruque JM, González-Martín KL, Dorado Calasanz C (1995) Langmuir 11:4515
21. Lu JR, Lee EM, Thomas RK, Penfold J, Flitsch SL (1993) Langmuir 9:1352
22. Schulz PC, Rodríguez JL, Morini MA, Puig JE (1996) Colloid Polym Sci, in press
23. Lu JR, Simister EA, Lee EM, Thomas RK, Rennie AR, Penfold J (1992) Langmuir 8:1837
24. Lu JR, Marrocco A, Su TJ, Thomas RK, Penfold J (1993) J Colloid Interface Sci 158:303
25. Clint JH (1992) Surfactant Aggregation. Blackie, Glasgow
26. Lu JR, Simister EA, Thomas RK, Penfold J (1993) J Phys Chem 97:6024
27. Eastone J, Dalton J, Rogeda P, Sharpe D, Dong J (1996) Langmuir 12(11): 2706
28. Lu JR, Li ZX, Smallwood J, Thomas RK, Penfold J (1995) J Phys Chem 99:8233
29. Lu JR, Hromadova M, Thomas RK (1993) Langmuir 9:2417
30. Cabane B, Duplessi R, Zemb T (1985) J Phys Chem 46:2161
31. Weil I (1966) J Phys Chem 70:133
32. Nilsson B (1957) J Phys Chem 61:1137
33. Simister EA, Thomas RK, Penfold J, Aveyard R, Binks BP, Cooper P, Fletcher PDI, Lu JR, Sokolowski A (1992) J Phys Chem 96:1383
34. Fowkes FM (1962) J Phys Chem 66:385
35. Joos P (1967) Bull Chem Soc Belg 76:591
36. Rodakiewiccz-Nowak J (1982) J Colloid Interface Sci 85:586
37. Rodakiewiccz-Nowak J (1982) J Colloid Interface Sci 84:532
38. Rodakiewiccz-Nowak J (1983) Colloids Surfaces 6:143
39. Lucassen-Reynders EH (1976) Progr Surf Membr Sci 10:253
40. Schulz PC, Gschaider de Ferreira ME, Sierra GL (1995) Colloid Polym Sci 273:439
41. Ly LAN, Carbonell RG, McCoy BJ (1979) AIChE J 25(6):1015
42. LaMer VK (ed) (1962) Retardation of Evaporation by Monolayers. Academic Press, New York
43. LaMer VK, Healy TW (1965) Science 148:36
44. Caskey JA, Barlage WB (1972) J Colloid Interface Sci 41:52
45. Mihara Y (Sep 12, 1966) Chem Eng News 20
46. McCoy BJ (1982) AIChE J 28(5):844